Journal of Chromatography, 259 (1983) 433–444
Elsevier Science Publishers B.V., Amsterdam — Printed in The Netherlands

CHROM. 15,591

GAS–SOLID CHROMATOGRAPHIC CHARACTERIZATION OF ACTIVE CARBONS

A. BETTI*, F. DONDI, G. BLO and S. COPPI
Cattedra di Chimica Analitica, Istituto Chimico dell'Universitá, via Borsari, 46, I-44100 Ferrara (Italy)
G. COCCO
Istituto di Chimica Fisica, Universitá di Venezia (Italy)
and
C. BIGHI
Cattedra di Chimica Analitica, Universitá di Ferrara (Italy)
(Received November 8th, 1982)

SUMMARY

The characterization of two active carbons was carried out by using gas chromatographic (GC) peak parameters (mean and variance) obtained by fitting experimental data with the Edgeworth–Cramér series. These results were then compared with those obtained from mercury porosimetry, low-temperature nitrogen adsorption measurements, small-angle X-ray diffraction, scanning electron microscopy and transmission electron microscopy. With regard to mass exchange processes, the chromatographic technique yields results which agree with those obtained by the other techniques. In regard to adsorption capacity, the GC characterization is more direct and unambiguous.

INTRODUCTION

It has been known for some time that gas chromatography (GC) can be used to determine the thermodynamic, kinetic and transport properties of porous, adsorbent materials[1–5]. Most works have assumed that the chromatographic profile is Gaussian in form and on this basis the peak parameters (maximum and band dispersion) are calculated.

However, under the experimental conditions normally used (columns of limited length and materials of large particle size), the peaks are far from Gaussian in form and the peak parameters are calculated from statistical moments determined by integration techniques[6]. This procedure, although quite rapid, leads to inaccurate and imprecise results[7–11].

Better results are obtained by fitting experimental data to theoretical models such as the Gram–Charlier Series of Type A[7,12] or the Poisson law[13]. Recently[14], the Edgeworth–Cramér (EC) Series was shown to be more efficient than the Gram–

0021-9673/83/$03.00

Charlier Series in fitting chromatographic peaks obtained under conditions of infinite dilution and characterized by notable asymmetry. Furthermore, it was verified that this procedure permits the statistical peak parameters to be determined accurately provided that specific conditions are respected (linear chromatographic isotherm and a sufficiently high degree of expansion of the series used for fitting)[15,16].

In the present work, an unbiased method is employed to determine chromatographic peak statistical parameters, and the chromatographic characterization of commercial active carbons thus obtained is compared with the results of other physical and chemical-physical techniques such as mercury porosimetry, scanning electron microscopy (SEM), transmission electron microscopy (TEM), small-angle X-ray scattering (SAXS) and low-temperature nitrogen adsorption (BET). The purpose of this study is to determine the advantages and disadvantages of the chromatographic technique in identifying the characteristics of complex porous materials.

EXPERIMENTAL AND CALCULATIONS

Chromatographic measurements

The chromatographic apparatus, the method of obtaining data and the columns have already been described[14].

The commercial active carbons (30–40 mesh) were R-2 Extra (A carbon) (Norit, Milan, Italy) and S-2 (B carbon) (Bonaccorsi, Ferrara, Italy). The hydrocarbons (C_1–C_4) (99.6%, J. T. Baker) were injected into the column in a helium or nitrogen mixture using a 0.2-ml gas valve (Bimatic; Carlo Erba, Milan, Italy). In the most unfavourable cases the contribution of this type of injection to band broadening was less than 2% of the total chromatographic peak dispersion and was, therefore, not taken into consideration.

A soap bubble flow meter fitted with photoelectric cells and an electronic timer (Seac, Firenze, Italy) was used to measure the flow of the transport gases helium and nitrogen (IGT, Pisa, Italy). The column pressure drop was measured with a mercury differential manometer, while output pressure (equal to atmospheric pressure) was determined with a Fortin barometer.

The size of the column was taken into consideration in calculating both the linear flow-rate and the correct retention volume. A value of 0.4 was assumed for the intraparticle and interparticle porosity[17].

For stability of peak shape parameters, obtained according to the described method[14], the EC series was expanded to the 7th degree, but for the R-2 Extra samples, expansion to the 4th degree was sufficient. Under the experimental conditions adopted the retention volume was independent of the carrier gas and was constant to ± 1% upon variation in the sample amount and in carrier flow-rate (Table VII of ref. 14). These results enable the specific retention volumes to be correlated with the Henry constant[2].

The mass transport coefficients of *n*-butane and isobutane were obtained by the Schettler and Giddings method[18] using the formula of Fuller *et al.*[19] to calculate the adsorbate diffusion coefficient.

Mercury porosimetry and electron microscopy

A Carlo Erba Series 1500 mercury porosimeter was employed. A cylindrical form was adopted[20] in calculating the size (radius) of the pores (Fig. 1).

For scanning electron microscopy (SEM) a Siemens Autoscan was utilized. The samples were covered with a gold film by means of an Edwards S 150 metallizer. The electron angle of incidence was 35°. Transmission electron microscopy were carried out with a Siemens 101 Elmiskop.

Surface area measurements by SAXS and BET

The X-ray intensities were collected with a Kratky camera adjusted to the "infinite" beam condition and equipped with an electronic step-scanner. Nickel-filtered Cu-K_α radiation with a pulse-height discriminator was used. The data were placed on an absolute scale by the moving slit technique[21]. A more detailed description of the methods used for determining the total surface area and the pore size distribution has already been reported[22].

The specific surface area, S_{sp} (m^2 g^{-1}), can be derived from the asymptotic behaviour in the tails of small angle absolute intensities according to the relationship[23]

$$S_{sp} = 10^4 \cdot \frac{16\pi^2 \lim_{m \to \infty} m^3 J(m)}{a^2 \lambda^4 r_e^2 N_A^2 P_0 (\Delta p)^2 p} \tag{1}$$

where $J(m)$ is the slit-smeared intensity (n_e^2 pulses per second per cm^2, n_e being the number of electrons), m is the instrumental variable defined in direct space as the distance (cm) between the primary intensity and the diffracted ray on the recording plane, a is the distance (cm) between the sample and the recording plane, λ is the

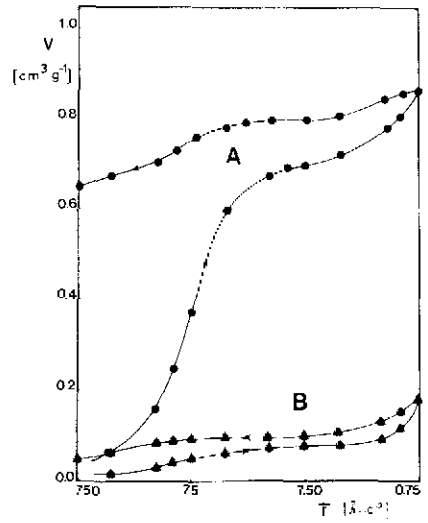

Fig. 1. Mercury porosimetry diagrams of R-2 Extra (A) and S-2 (B) active carbons.

X-ray wavelength (cm), r_e^2 is the Thomson factor (cm^2), N_A is Avogadro's number, P_0 is the energy coming from the focus and arriving along 1 cm in the plane of registration (pulses sec^{-1} cm^{-1}), Δp is the electron-density difference between the two phases in the scattering system (n_e per cm^3) and p is the sample "thickness" (g cm^{-2}).

Although eqn. 1 does not depend on any arbitrary assumption, the magnitude of the interfacial surface is not representative of the pore size distribution within the scattering system. To gain this kind of structural information the whole angular scattered intensity has to be considered and, under certain conditions[24,25], can be approximately regarded as the sum of the intensities diffused by the individual heterogeneities, according to

$$I(h) = (\Delta p)^2 \int_0^\infty D_V(R) R^{-3} V^2(R) i_0(hR)\, dR \qquad (2)$$

where $I(h)$ is the intensity deconvoluted from collimation effects, h is the modulus of the diffraction vector, $4\pi\lambda^{-1} \cdot \sin\theta$ with 2θ the scattering angle, $D_V(R)$ is the volumetric distribution function which describes the volume of all pores defined by the size parameter, R, and $i_0(hR)$ is the intensity scattered by a single heterogeneity with radius R and volume $V(R)$.

The analytical solution of $D_V(R)$ in eqn. 2 is accomplished by least-squares fitting of the intensity calculated on the basis of a specific structural model to the observed profile. The application of this method suffers from some limitations arising from the ambiguity of assuming a particular pore-matter model[26] and because of the nature of heterogeneities in closely packed carbon and which are probably not uniform in shape. However, in the present case, the essential features of the calculated pore distribution functions provide an interesting comparison of the underlying characteristics of the samples under study.

In the manipulation of eqn. 2 to get $D_V(R)$ curves, a number of explicit expressions are available. These expressions differ in the shape model of the scattering entities. Nevertheless the best fitting was obtained for the spherical approximation. The distribution functions thus obtained were checked by making use of a second analytical method, derived from Debye's correlation function, via a Fourier–Bessel transformation of the smeared intensities[27]. Although the two methods differ largely in regard to the theoretical approaches, the agreement obtained between the results underlines the reliability of the main details of the reported distribution functions.

The results of surface area measurements are reported in Table I, while the relative scattering intensities and the size distribution curves are presented in Figs. 2 and 3. Table I also reports the BET surface area and the micropore volume, determined according to Broekhoff and De Boer[28,29].

RESULTS AND DISCUSSION

Physical characteristics

The mercury porosimetry measurements and electron microscopy investigations provided a detailed description of the geometric structure of these materials. Porosimetry and SEM microscopy can be directly compared and furnish information

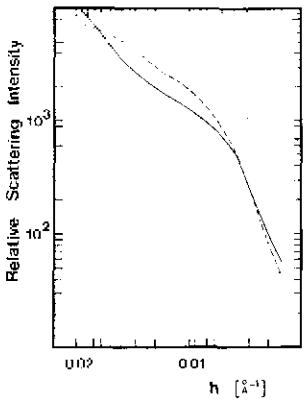

Fig. 2. The relative scattering intensities *versus* h for R-2 Extra; (———) and S-2 (– – –).

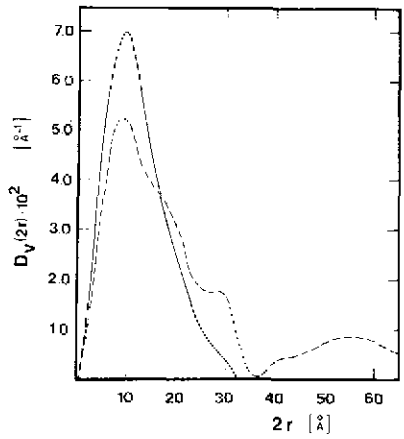

Fig. 3. The size distribution curves *versus* the inhomogeneity diameter for predominantly micropores. ———, R-2 Extra; – – –, S-2. Void distribution curves were obtained according to eqn. 2.

about pores of size greater than 200 Å. Figs. 4 and 5 (SEM) show how the two carbons studied differ structurally. The A carbon (R-2 Extra) is a conglomerate of finer particles (0.2–2 μm) endowed with an extensive structure and a complex network of small canals inside the grain, while the B carbon (S-2) appears compact with clean-cut fracture surfaces. The mercury porosimetry (Fig. 1) indicates that the A carbon has a system of pores of sizes ranging between 10,000 and 5000 Å. These pores contribute to an interconnected interparticle porosity of the order of 0.5 cm^3 g^{-1}. This type of porosity is absent in the B carbon. These observations lead to the classification of the two types of carbons as "wood charcoal" (A) and "coconut charcoal" (B). TEM microscopy (Fig. 6) allows one to examine part of the transitional porosity (2000–50 Å). Within this range of pore sizes, the A carbon appears to be more homogeneous and does not reveal pores of sizes from 100 to 1000 Å. On the other hand, the B carbon demonstrates a rich and varied porous structure within the same size range.

The above observations permit the first material (A) to be classified as an active carbon which gives rise to a rapid exchange of mass, more appropriate for liquid phase adsorption, while the second carbon (B) is more suitable for gas phase adsorption where the diffusion coefficient of the adsorbate is higher[30,31]. However, it is the notable microporosity and high specific surfaces of active carbons which de-

TABLE I

SPECIFIC SURFACE AREA, S_{sp} AND PORE VOLUME V_p

Carbon	S_{sp} (m^2 g^{-1})		V_p (cm^3 g^{-1})
	SAXS	*BET*	
R-2 Extra	1184	1140	0.381
S-2	997	867	0.309

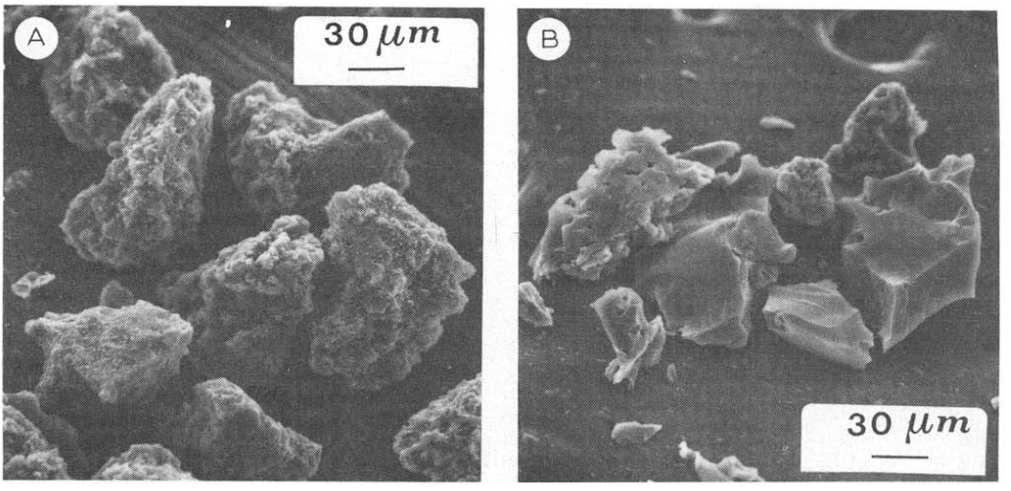

Fig. 4. Scanning electron microscopy of R-2 Extra (A) and S-2 (B).

termine their great capacity for adsorption and which, nevertheless, cannot be established by the techniques examined so far.

The SAXS and BET techniques give comparable surface areas for these materials (Table I), although both furnish higher (10%) values for the R-2 Extra (A carbon).

It remains to be pointed out that the most convincing and unequivocal data available are those in regard to the macroporous geometric structure, and that both SEM and mercury porosimetry supply consistent and convincing descriptions. In contrast, some limitations must be placed on the interpretation of the TEM data, since this technique does not permit a quantitative evaluation of the degree of S-2 (B carbon) porosity interconnection. Greater uncertainty in the classification of active

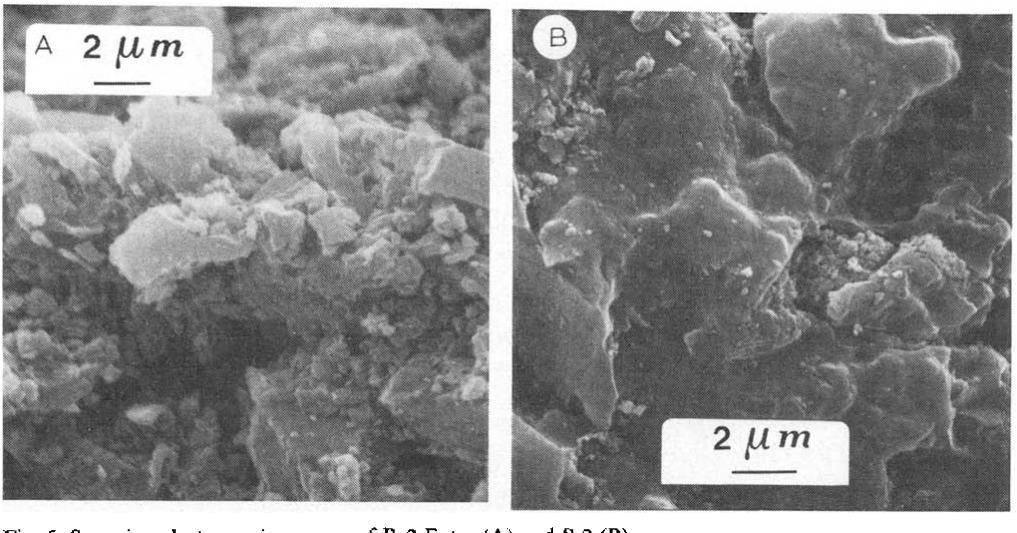

Fig. 5. Scanning electron microscopy of R-2 Extra (A) and S-2 (B).

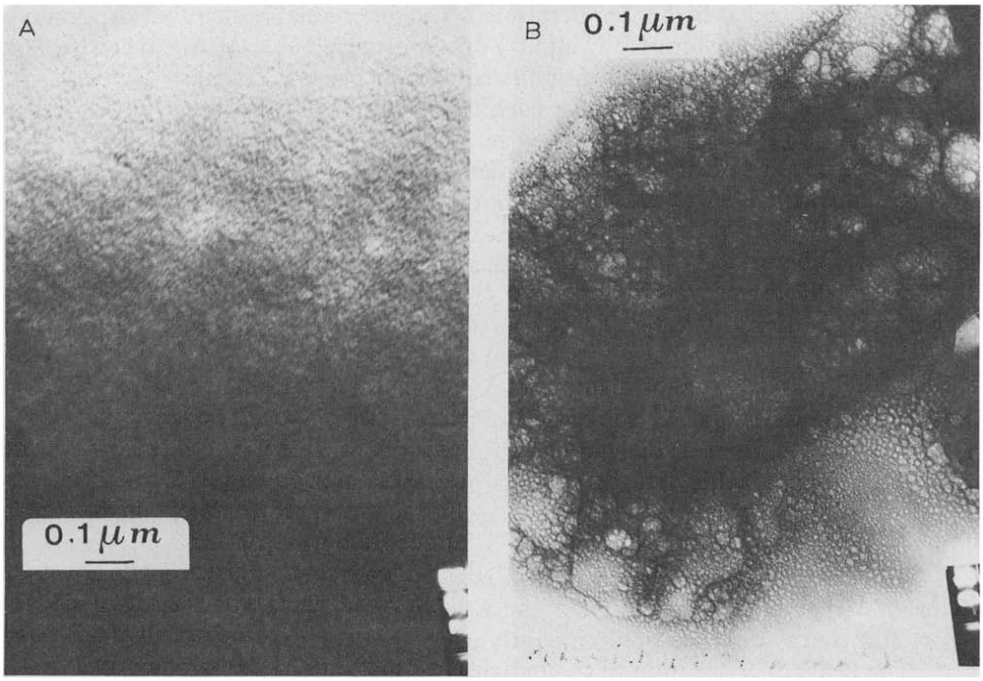

Fig. 6. Transmission electron microscopy of R-2 Extra (A) and S-2 (B).

carbons exists when specific surface areas obtained by the SAXS and BET techniques are evaluated.

Now let us turn to the conclusions which can be drawn from thermodynamic and kinetic data obtained by gas chromatography by means of parameter determination using EC series.

Retention and heat adsorption parameters

The specific retention volumes, calculated at 0°C and relative to 1 g of active carbon, are reported in Table II. Fig. 7, shows ln V_g, limited to *n*-alkanes at a single temperature of 160°C, as a function of the number of carbon atoms (for *n*-C_4 the data were extrapolated

TABLE II

SPECIFIC RETENTION VOLUMES, V_g (ml g^{-1})

Compound	*R-2 Extra*					*S-2*				
	140°C	*160°C*	*180°C*	*220°C*	*240°C*	*140°C*	*160°C*	*180°C*	*220°C*	*240°C*
CH_4	5.2	4.3	—			2.5	2.0	—		
C_2H_6	44.9	30.8	—			15.7	11.1			
C_2H_4	33.4	23.5	—			12.5	9.0	—		
C_3H_8	475	272	142			96.6	59.9	36.6		
C_3H_6	421	241	126			88.7	55.0	33.5		
n-C_4H_{10}				267	158				61.8	35.4
iso-C_4H_{10}				202	125				49.1	29.4

from those obtained at higher temperatures). The differential heats of adsorption obtained from the relationship of ln V_g and $1/T$ are reported in Table III, together with data obtained by other authors[32] for graphitized carbon black (GTCB).

Examination of the results for each carbon studied reveals the following:

(a) a linear relationship between ln V_g and the number of *n*-alkane carbon atoms. For *n*-C_4 and iso-C_4 the elution order is in agreement with their boiling points;

(b) the differential heat of adsorption for *n*-alkanes steadily increases with increasing carbon number (average increase = 3.3 kcal mol^{-1});

(c) the adsorption heats for alkenes are lower or quite similar to those of the corresponding *n*-alkanes.

The linear relationships between ln V_g and the corresponding molar heat of adsorption and carbon number suggest that the two active carbons have no molecular sieving effect, at least in respect of the types of adsorbate used in this study[33].

The retention volumes and heats of adsorption of alkenes are in agreement with the lower polarizability of these molecules in comparison to the corresponding *n*-alkanes. Furthermore, the heats of adsorption indicate that the active carbon surfaces do not possess centres capable of specific interaction with the alkene molecules[2,33].

The average increase in adsorption heat in the *n*-alkane series is characteristic of the first type of adsorbent under the Kiselev and Yashin classification[2] where adsorption energy depends predominantly on dispersive interactions.

The heats of adsorption of the individual hydrocarbons are higher than those obtained, by GC, on graphitized carbon black (GTCB) (Table III). This difference is justified by the microporous structure of the examined materials[31,34]. The ratio of the value of the hydrocarbon adsorption potential on active carbons, Φ_{0A}, to that on graphitized carbon black, Φ_{0G}, calculated according to Stoeckli[35] (Table IV), is in agreement with values reported by other authors[36] for different types of active carbons.

The chromatographic data indicate clearly that type A carbon has a greater adsorption capacity than type B. However, this has not been verified by the uncertain surface areas obtained by SAXS and BET.

Efficiency curves and mass transfer coefficients

The efficiency of the active carbon columns under examination is illustrated in Fig. 8 where the height of the theoretical plate, H (cm), for *n*-butane is expressed as

TABLE III

HEATS OF ADSORPTION (kcal mol^{-1})

Compound	*R-2 Extra*	*S-2*	*GTCB*[32]
CH_4	3.6	3.9	3.11
C_2H_6	6.7	6.3	4.53
C_2H_4	6.3	5.8	4.30
C_3H_8	11.0	9.0	5.93
C_3H_6	11.2	9.0	—
n-C_4H_{10}	13.2	14.0	7.21
iso-C_4H_{10}	12.0	12.8	6.95

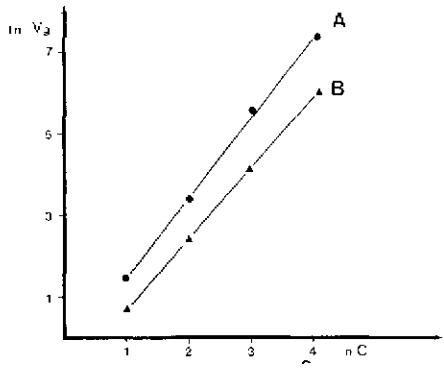

Fig. 7. Relationship between ln V_g and carbon number nC for *n*-alkanes at 160°C on (A) R-2 Extra and (B) S-2 active carbons.

a function of the helium and nitrogen flow-rate (cm sec^{-1}) at 240°C. The curves are obtained at high rates where the expression proposed by Grubner[6] for columns of porous materials approaches the equation of a straight line whose slope is the global coefficient of mass transfer

$$C = 2\,R^2/15\,\varphi\,D_r K_c \tag{3}$$

where R = packing particle radius, D_r = radial diffusion coefficient, K_c = bulk adsorption equilibrium constant and φ = ratio between internal and external porosity. The regression parameters of the fitting of the curves according to $H = a\,u + b$ and the ratio ρ of the a coefficients obtained for nitrogen and helium are reported in Tables V and VI.

Examination of the regression coefficients shows that the mass transfer process is much slower for S-2 (B carbon). Furthermore, the process is practically independent of adsorbate nature. The b terms are a measure of the effect of eddy diffusion and, if they are a characteristic of the column rather than of the material[5,6], indicate that for S-2 carbon the adsorbate molecules are obliged to follow a much more tortuous course during the transport process. The ρ values can be correlated to the

TABLE IV

ADSORPTION POTENTIALS OF HYDROCARBONS ON ACTIVE CARBONS, Φ_{0A}, AND ON GRAPHITIZED CARBON BLACK (GTCB), Φ_{0G}

Compound	*R-2 Extra*		*S-2*		*GTCB*
	$-\Phi_{0A}$	Φ_{0A}/Φ_{0G}	$-\Phi_{0A}$	Φ_{0A}/Φ_{0G}	$-\Phi_{0G}$
CH_4	2.3	0.86	2.6	0.98	2.67
C_2H_6	5.4	1.36	5.0	1.27	3.95
C_2H_4	5.0	1.34	4.5	1.21	3.72
C_3H_8	9.7	1.86	7.7	1.48	5.21
n-C_4H_{10}	11.7	1.87	12.5	2.00	6.23
iso-C_4H_{10}	10.5	1.75	11.3	1.89	5.97

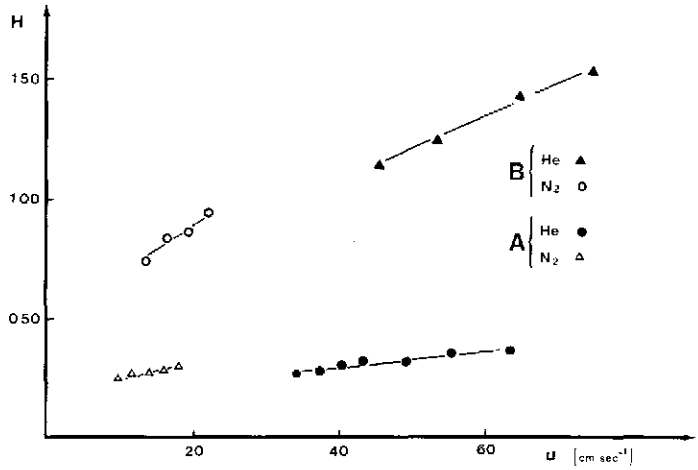

Fig. 8. Plots of H (cm) *versus* u (cm sec^{-1}) for n-butane at 240°C on (A) R-2 Extra and (B) S-2 active carbons.

ratio of the radial diffusion coefficients in helium and nitrogen respectively. Tables V and VI indicate that for R-2 Extra (A carbon) the mass transfer process is more strongly dependent on the nature of the carrier gas, compared with the other active carbon. Therefore, for this carbon the mass transport process occurs predominantly in the gas phase.

One interpretation of these results can be drawn from the Bosanquet interpolation formula for calculation of diffusion in porous systems. When the pore radius increases according to the cylindrical pore formula, the radial diffusion coefficient, D_r, approaches the value of the gas phase diffusion coefficient, D_g

$$D_r^{-1} = D_g^{-1} + D_k^{-1} \tag{4}$$

where D_k is the Knudsen diffusion coefficient[37,38]. When compared with the value

TABLE V

LINEAR FITTING ACCORDING TO $H = au + b$ FOR n-BUTANE IN HELIUM AND NITROGEN AT 220°C AND 240°C

Carbon	*Carrier*	$10^3 \cdot a$	b	$\rho = \frac{a(N_2)}{a(He)}$
R-2 Extra (240°C)	He	3.1 ± 0.2	0.15 ± 0.01	2.7
	N_2	8.5 ± 0.2	0.17 ± 0.02	
R-2 Extra (220°C)	He	3.5 ± 0.2	0.14 ± 0.01	1.8
	N_2	6.4 ± 0.1	0.18 + 0.01	
S-2 (240°C)	He	14 ± 3	0.41 ± 0.06	1.3
	N_2	18 ± 5	0.34 ± 0.02	
S-2 (220°C)	He	14 ± 1	0.42 ± 0.04	1.3
	N_2	18 ± 2	0.35 ± 0.02	

TABLE VI

LINEAR FITTING ACCORDING TO $H = au + b$ FOR ISOBUTANE IN HELIUM AND NITROGEN AT 220°C AND 240°C

Carbon	*Carrier*	$10^3 \cdot a$	b	$\rho = \frac{a(N_2)}{a(He)}$
R-2 Extra (240°C)	He	3.4 ± 0.5	0.16 ± 0.02	2.4
	N_2	8.3 ± 0.1	0.18 ± 0.02	
R-2 Extra (220°C)	He	3.6 ± 0.1	0.14 ± 0.01	1.9
	N_2	6.7 ± 0.1	0.17 ± 0.01	
S-2 (240°C)	He	17 ± 1	0.37 ± 0.08	1.3
	N_2	23 ± 4	0.41 ± 0.07	
S-2 (220°C)	He	17 ± 1	0.34 ± 0.01	1.2
	N_2	21 ± 1	0.37 ± 0.01	

of the diffusion coefficient ratio in the gas phase, D_g(helium)/D_g(nitrogen) = 3.2 for the two temperatures and the two adsorbates, the ρ values of R-2 Extra carbon show that this material is characterized by high macroporosity. The solid phase mass transfer coefficients, C_s[39], Table VII, evaluated on the basis of the Giddings theory, indicate how much more rapidly the conditions of adsorption equilibrium are reached for R-2 Extra, again consistent with its macroporous structure.

TABLE VII

MASS TRANSFER COEFFICIENTS, C_s (msec)

Temperature (°C)	*R-2 Extra*	*S-2*
n-Butane		
240	0.21 ± 0.06	9.8 ± 0.2
220	1.8 ± 0.2	14.9 ± 0.2
Isobutane		
240	1.4 ± 0.05	12.3 ± 0.2
220	2.8 ± 0.2	19.0 ± 0.3

CONCLUSIONS

A comparison of the data obtained from traditional physical techniques and from GC by use of the EC series demonstrates that characterization of the adsorption capacity by gas chromatography is without doubt the more direct and unambiguous. By varying the type of solute it is possible to examine the nature and the adsorbent capacity of active carbon surfaces in greater detail, while measurement of surface areas by techniques such as BET and SAXS is difficult to evaluate, of limited application and laborious.

The GC, mercury porosimetry and SEM techniques all indicate the important rôle of macroporosity in the exchange of mass between two phases, while the TEM technique and the analysis of chromatographic band broadening do not give unambiguous results. Therefore, the GC characterization of such complex porous adsorbents as the active carbons is not inferior to that obtained with alternative, more time-consuming techniques.

ACKNOWLEDGEMENTS

The authors would like to thank M. Chiarioni (CNR, Genova) for the mercury porosimetry measurements, C. Cometto (C. R. G. Natta-Montedison, Ferrara) for the BET surface area measurements, G. Martinelli (Istituto di Fisica, University of Ferrara) and the Center for Electron Microscopy of the University of Ferrara for the SEM and TEM measurements.

This work was supported by the National Research Council of Italy (CNR), Programma Finalizzato "Promozione della Qualitá dell'Ambiente-Sottoprogetto Acqua-IRSA", Contribution No. 80.01716.

REFERENCES

1 H. W. Habgood, in E. A. Flood (Editor), *Chromatography and the Solid–Gas Interface*, Marcel Dekker, New York, 1967, Ch. 20, p. 611.
2 A. V. Kiselev and Y. I. Yashin, *Gas-Adsorption Chromatography*, Plenum, New York, 1969.
3 M. Suzuki and J. M. Smith, *Advan. Chromatogr.*, 13 (1965) 213.
4 J. R. Conder and C. L. Young, *Physicochemical Measurements by Gas Chromatography*, Wiley, New York, 1979.
5 J. C. Giddings, *Dynamics in Chromatography, Part I, Principles and Theory*, Marcel Dekker, New York, 1965.
6 O. Grubner, *Advan. Chromatogr.*, 6 (1968) 173.
7 C. Vidal-Madjar and G. Guiochon, *J. Chromatogr.*, 142 (1977) 61.
8 S. N. Chesler and S. P. Cram, *Anal. Chem.*, 43 (1971) 1922.
9 S. N. Chesler and S. P. Cram, *Anal. Chem.*, 44 (1972) 2240.
10 T. Petitclerc and G. Guiochon, *Chromatographia*, 8 (1975) 185.
11 S. D. Mott and E. Grushka, *J. Chromatogr.*, 148 (1978) 305.
12 D. A. McQuarrie, *J. Chem. Phys.*, 38 (1963) 437.
13 J. Villermaux, *J. Chromatogr.*, 83 (1973) 205.
14 F. Dondi, A. Betti, G. Blo and C. Bighi, *Anal. Chem.*, 53 (1981) 496.
15 D. Dondi, *Anal. Chem.*, 54 (1982) 473.
16 F. Dondi, *Proceedings of the IV Congresso Nazionale della Divisione di Chimica Analitica, Urbino, Sept. 6–9, 1982.*
17 O. Grubner, M. Ralek and A. Zikánová, *Collect. Czech. Chem. Commun.*, 31 (1966) 852.
18 P. D. Schettler and J. C. Giddings, *Anal. Chem.*, 36 (1964) 1483.
19 E. N. Fuller, P. D. Schettler and J. C. Giddings, *Ind. Eng. Chem.*, 58 (1966) 19.
20 S. J. Gregg and K. S. W. Sing, *Adsorption Surface Area and Porosity*, Academic Press, New York, 1969, p. 182.
21 H. Stabinger and O. Kratki, *Makromol. Chem.*, 179 (1978) 1655.
22 G. Cocco, L. Schiffini, G. Strukul and G. Carturan, *J. Catal.*, 65 (1980) 348.
23 A. Guinier and G. G. Fournet, *Small Angle X-Ray Scattering*, Wiley, New York, 1955.
24 C. G. Vonk, *J. Appl. Crystallogr.*, 9 (1976) 433.
25 R. Perret and W. Ruland, *J. Appl. Crystallogr.*, 4 (1971) 444.
26 W. Vogel and R. Hosemann, *Vth International Conference on Small Angle Scattering, Berlin, October 1980*, Contribution P IV 24.
27 J. R. Donati, B. Pascal and A. J. Renouprez, *Bull. Soc. Fr. Mineral. Crystallogr.*, 90 (1967) 452.
28 J. C. P. Broekhoff and J. H. De Boer, *J. Catal.*, 9 (1967) 8.
29 J. C. P. Broekhoff and J. H. De Boer, *J. Catal.*, 9 (1967) 15.
30 E. T. Turkdogan, R. G. Olsson and J. V. Vinters, *Carbon*, 8 (1970) 545.
31 M. M. Dubinin, in P. L. Walker, Jr. (Editor), *Chem. Phys. Carbon*, 2 (1966) 56.
32 E. V. Kalaschnikova, A. V. Kiselev, R. S. Petrova and K. D. Scherbakova, *Chromatographia*, 4 (1971) 595.
33 V. Patzelová, O. Kadlec and P. Seidl, *J. Chromatogr.*, 91 (1974) 313.
34 D. H. Everett and J. C. Powl, *J. Chem. Soc., Farad. Trans. 1*, 72 (1979) 619.
35 H. F. Stoeckli, *Chimia*, 28 (1974) 645.
36 A. Perret and F. Stoeckli, *Helv. Chim. Acta*, 58 (1975) 2318.
37 R. B. Evans and G. M. Watson, *J. Chem. Phys.*, 33 (1961) 2076.
38 A. Zikánová, *J. Chromatogr. Sci.*, 9 (1971) 248.
39 W. R. MacDonald and H. W. Habgood, *Can. J. Chem. Eng.*, 50 (1972) 462.